

# Experimental Study on Passive Earth Pressure against Flexible Retaining Wall with Drum Deformation

Xinnian Zhu, Yongqing Zeng, *Member, IAENG*, Weidong Hu, Xiaohong Liu, and Xiyu Zhou

**Abstract**—In order to analyze failure characteristics and passive earth pressure distribution pattern against flexible retaining wall with drum deformation, a series of laboratory model tests using particle image velocimetry technique and earth pressure measurement of sandy soil with different limited width were conducted based on the self-made model equipment. The particle image velocimetry technique was employed to observe the development of failure zone in the sandy soil, the results show that the failure surface in the limited width soil is a continuous and curved surface in the drum deformation mode when the passive soil mass closes to or reaches limit state, the failure surface intersects wall body without passing through the heel. Earth pressure test results show that with the increase of lateral displacement, the distribution and variation of passive earth pressure are significantly different; the horizontal passive earth pressure behind flexible retaining wall presents a nonlinear drum distribution along the wall body; in the vicinity of the maximum horizontal displacement of flexible retaining wall, the earth pressure increases obviously and keeps increasing rapidly. Within finite width, the width to height ratio of sandy soil is smaller, the peak passive earth pressure of retaining wall is higher. Under the condition of same width to height ratio, the peak passive earth pressure is larger with the increase of the embedded depth of retaining wall. The analysis results can provide reference for design and construction of flexible retaining structure such as row pile, sheet pile and diaphragm wall.

**Index Terms**—limited soil, passive earth pressure, flexible retaining wall, drum deformation

Manuscript received July 25, 2020; revised February 9, 2021. The study was supported by the Natural Science Foundation of Hunan Province, China (Grant No. 2017JJ2110), the Program of Hunan Province Education Department, China (Grant No.19C0870) and the Key Scientific Program of Hunan Education Department, China (Grant No. 20A228).

Xinnian Zhu is a lecturer in College of Civil Engineering and Architecture, Hunan Institute of Science and Technology, Yueyang, 414000, China (e-mail: 11999496@hnist.edu.cn).

Yongqing Zeng is a lecturer in College of Civil Engineering and Architecture, Hunan Institute of Science and Technology, Yueyang, 414000, China (corresponding author e-mail: 1013433575@qq.com).

Weidong Hu is a professor in College of Civil Engineering and Architecture, Hunan Institute of Science and Technology, Yueyang, 414000, China (e-mail: 11996498@hnist.edu.cn).

Xiaohong Liu is a professor in College of Civil Engineering and Architecture, Hunan Institute of Science and Technology, Yueyang, 414000, China (e-mail: 11991491@hnist.edu.cn).

Xiyu Zhou worked as an assistant engineer in China Railway Major Bridge Engineering Group Limited Company, Wuhan 430050, China (e-mail: 14162601465@vip.hnist.edu.cn).

## I. INTRODUCTION

In municipal projects such as subway station, underground pipeline trench and urban basement construction, a large number of narrow and long foundation pits have appeared, the flexible retaining structure such as row pile, sheet pile and diaphragm wall have been widely used in the narrow and long foundation pit[1]. When flexible retaining structure is stressed, it will produce deflection deformation because the thickness of the flexible retaining structure is very small compared with the length, the stress and deformation distribution law of flexible retaining wall are obviously different from that of rigid retaining wall[2]. According to the classical Coulomb and Rankine earth pressure theory [3,4], the earth pressure of flexible retaining structure cannot be accurately calculated.

When the soil is excavated in a long and narrow foundation pit, the passive earth pressure is affected not only by the horizontal displacement, but also by the displacement pattern[5,6]. As an effective and common form of support for narrow and long foundation pit, the bottom of flexible retaining wall is embedded in rock or soil used as a fixed fulcrum and the top of flexible retaining wall is supported or anchored by an internal support or anchor rod. In the process of earthwork excavation, the flexible retaining wall gradually bends to the interior of foundation pit, the top and bottom deformation of flexible wall is very small for fixed constraint effect, meanwhile, the middle part of flexible wall bulges into the foundation pit; therefore, the displacement mode becomes a typical drum deformation mode. The failure characteristics and passive earth pressure distribution of finite width soil in drum deformation mode for flexible retaining wall in long and narrow foundation pit directly affects the calculation accuracy on the bottom passive resistance of the foundation pit; therefore, experimental study on passive earth pressure against flexible retaining wall with drum deformation has important engineering design and application significance.

At present, the distribution law on active earth pressure of rigid retaining wall in infinite soil under three modes: translation, rotation around the toe of wall, and rotation around the top of wall have been studied through model tests [7-10]. Ying [11,12] studied active earth pressure of flexible retaining wall in arbitrary displacement and proposed the calculation method of earth pressure distribution and height of resultant force action point by simplifying soil into the

combination of nonlinear springs and a rigid plasticity object; In terms of the drum deformation mode of flexible retaining wall, the mathematical formula on active earth pressure strength, resultant force and action point of resultant force are derived through theoretical analysis, the relevant theoretical results are compared with experimental results and Coulomb earth pressure theory. Based on Mononobe-Okabe's postulation, Peng [13] set up the first-order differential equation for passive earth pressure on the retaining wall for the translation(T) mode, movement modes of rotation around base(RB) and rotation around top (RT) by analyzing slice elements extracted from sliding soil wedge; the comparison between calculated results by the present formulas and Coulomb's theory show that the earth pressure is nonlinearly distributed and the distance from the action point of resultant pressure to the base of wall increases with the order of (RB) mode, (T) mode, and (RT) mode.

However, the boundary conditions of finite width soil formed by long and narrow foundation pit are obviously different from that of infinite soil. Take [14] and Khosravi [15] believed that the classical Coulomb and Rankine earth pressure theory would make the design results of retaining wall tend to be conservative by conducted a series of model tests on the active earth pressure of finite soil. Through model test, Xu[16] and Ying [17] studied passive earth pressure of rigid retaining wall with finite soil under translational mode, the passive earth pressure of limited width rigid retaining wall is larger than Coulomb passive earth pressure of infinite width retaining wall at arbitrarily depth; with the decrease of soil width, the passive earth pressure increase significantly.

The above studies show that the deformation and position of limit fracture plane for limited width soil is obviously different from semi-infinite space, in which the distribution characteristics of earth pressure and the acting point position of resultant force have changed. In the existing model tests, abundant researches on the distribution of active and passive earth pressure of rigid retaining wall under various displacement modes have been done; however, the calculation of earth pressure, especially the passive earth

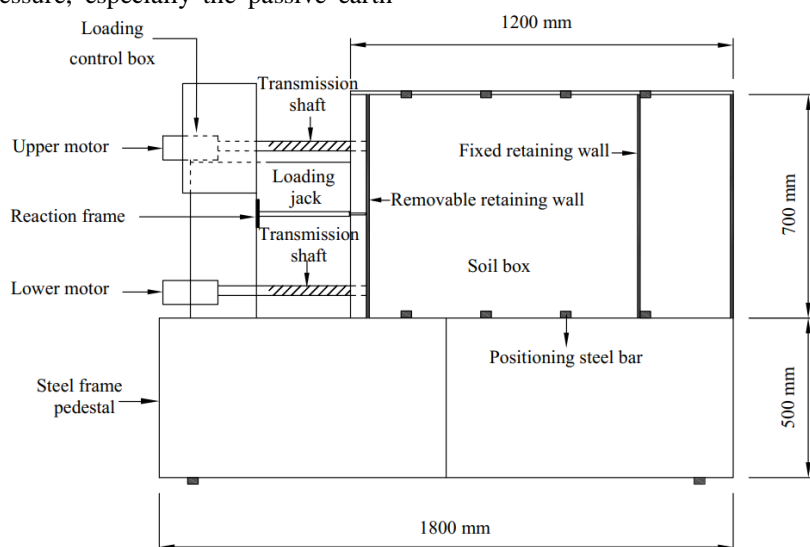
pressure of flexible retaining wall is insufficient. The flexible support such as row pile, sheet pile and diaphragm wall is widely used in excavation engineering, in order to analyze the distribution and variation characteristics of earth pressure and simulate central deflection of flexible retaining wall when the drum deformation occurs, a series of laboratory model tests using particle image velocimetry technique and earth pressure measurement about the sandy soil with different limited width were conducted, in which the earth pressure distribution law, deformation and failure characteristics of soil in the passive zone will be discussed, it provides a good reference for the calculation of earth pressure at the drum deformation of flexible retaining structure with finite width.

II. DESIGN AND MANUFACTURE OF TEST MODEL

The test was carried out with a self-made model box; the structure consists of four parts: soil box, transmission control system, particle image velocimetry (PIV) system and earth pressure measurement system. The model frame is made of stainless steel with tempered glass at the front and steel plate at the back.

A. Soil box for test model

In model tests, the cohesionless sand is taken as filling material, the schematic and physical diagram of model box is shown in Fig.1. The soil test is carried out in the soil box, which is divided into two parts: PIV imaging and earth pressure test. The inner dimension of soil box is 1200 mm long, 425 mm wide and 700 mm high. The fixed retaining wall is set in the right side of model box; the width of limited soil can be adjusted by setting the limit groove and baffle when fixed retaining wall is placed in the different parts of limit groove. The displacement of flexible retaining wall is realized by controlling the motor and loading jack in accordance with the loading control box. The maximum horizontal displacement of flexible retaining wall in drum deformation is measured by the upper and lower scales.



(a) The schematic diagram of model box



(b) The physical diagram of model box

Fig.1. The schematic and physical diagram of model box

The flexible retaining wall on the left side is made of polypropylene plate with 15 mm in thickness, 400 mm in width and 650 mm in height, which is used to simulate the support structure of foundation pit. The front side of polypropylene plate adopts double sided adhesive cloth base with sand to simulate completely rough surface of retaining wall, in order to ensure that the polypropylene plate can produce drum deformation position, there are 4 fixed supports in the upper and lower row on the reverse side; the fixed supports are made into goose shape with screw holes in the connecting part. The plate with a thickness of 10 mm, a width of 20 mm and a height of 120 mm is fixed at the contact part between polypropylene plate and loading jack to prevent local punching failure of polypropylene plate during deformation. The fixed retaining wall on the right side is made of 12 mm thick steel plate to simulate the fixed boundary of external wall for the existing underground structure, the surface of steel plate is not treated to simulate semi-rough contact state between concrete surface of underground structure and filling soil. The gaps between the left and right baffles, front and rear frame steel plate and tempered glass are sealed with soft wool stick; in addition, the frame steel plate and tempered glass are treated with lubricating oil.

**B. Transmission control system**

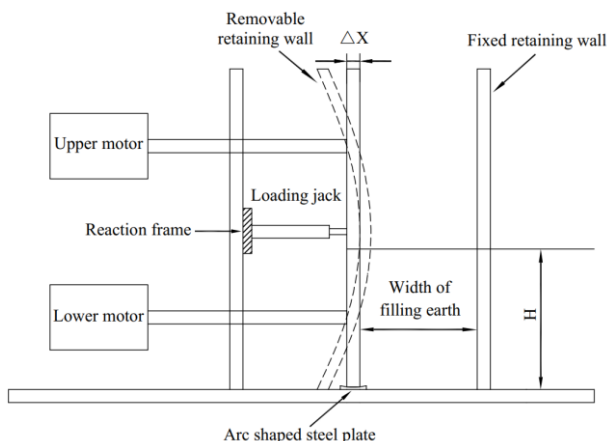


Fig. 2. Motion mode of flexible retaining wall with drum deformation

In order to simulate drum mode of flexible retaining wall such as row pile, sheet pile and diaphragm wall, Firstly, the upper and lower screws are driven by two motors to adjust the position of flexible retaining wall. Secondly, after positioning, sand is filled and flexible retaining wall is loaded with a central jack, where the top and bottom part is keeping fixed and middle part is keeping moving. Polypropylene plate has good flexibility to produce large deflection under the action of the jack. The maximum horizontal displacement of loading jack position is measured and the height of loading jack position is 228 mm, the soil in the box is squeezed to produce passive earth pressure. The drum deformation mode of flexible retaining wall is shown in Fig. 2.

**C. Particle image velocimetry test system**

Particle image velocimetry (PIV) is a non-intrusive optical measurement technique which allows capturing several thousand velocity vectors within large flow fields instantaneously in fractions of a second [18]. The PIV technique had emerged from laboratories to applications in fundamental and industrial research, in parallel to the transition from photographical to video recording techniques. the PIV technique has undergone further progress, in particular toward high-speed measurements and volumetric techniques capable of capturing all three components of the velocity vectors within a volume of the flow field instantaneously. Given the extreme versatility of PIV, the range of possible applications has drastically increased over the last three decades [19]. PIV is nowadays used in very different areas from aerodynamics to biology, from fundamental turbulence research to applications in the space station, from combustion to two-phase flows and in microfluidic devices. For many researchers and engineers, who are planning to utilize PIV for their special industrial or scientific applications, PIV is first and foremost an attractive tool with unique features, which they expect helping them to gain new insights in problems of mechanics.

The particle image velocimetry test system is shown in Fig. 3, the image acquisition and processing system based on PIV technology is composed of LED shadowless light source,

digital camera, computer and GOM Correlate image analysis software. The PIV test system can complete continuous photograph, image acquisition and image analysis. PIV technology takes a series of photos in real time with high-definition digital camera and uses GOM Correlate image analysis software to digitize all photos. Through continuous analysis of two consecutive digital images, the quantitative shear strain field and visual dynamic shear development process are obtained. During the passive earth pressure measurement, the PIV test system takes passive earth zone as analysis object, the soil displacement in the passive earth zone is obtained by using digital camera to take photos automatically with the shooting interval of 1-2 seconds and is analyzed by PIV analysis software. It should be known that the light source is placed on both sides of test equipment in order to reduce mirror reflection.

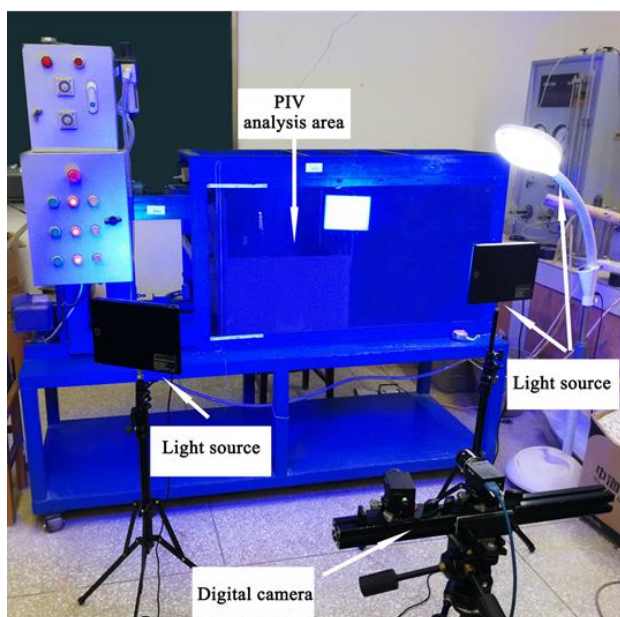


Fig. 3. Particle image velocimetry test system

D. Earth pressure measurement system

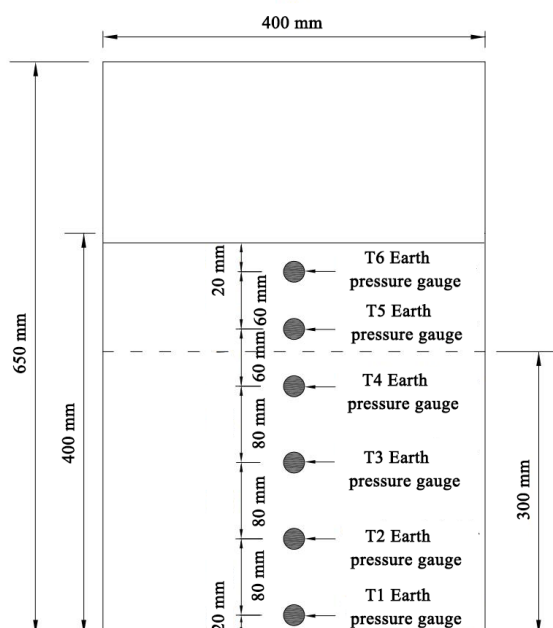


Fig. 4. Layout of earth pressure gauges

In the test, six earth pressure gauges (cyy9 type) with a range of 20-600 KPa were arranged on the side of flexible retaining wall near the foundation pit, the diameter and thickness of earth pressure gauge is 22 mm and 13 mm, respectively. The micro earth pressure gauge is embedded along the central line of polypropylene plate at different depths. Firstly, groove is formed at the corresponding position of polypropylene plate with the depth of 13 mm to ensure that the surface of earth pressure gauge is flush with the surface of flexible retaining wall. Secondly, holes at the edge of the groove are drilled to facilitate the wire of earth pressure gauge lead out. The location and depth of earth pressure gauges are shown in Fig. 4. The parameter calibration of earth pressure gauge usually has two methods: water calibration and sand calibration; in this test, the sand calibration is used, in which the loading curve of sand calibration is obtained by loading on the top surface of soil box.

During the test, the maximum horizontal displacement of flexible retaining wall at the loading jack position is tracked and measured by using the upper and lower positioning scales. After loading to a level of horizontal displacement, the maximum horizontal displacement value of filling soil  $\Delta x$  is recorded; the earth pressure value under this level of horizontal displacement is measured and averagely calculated by using data acquisition instrument.

E. Arrangement scheme for test

The physical and mechanical indexes of sand are as follows: particle size range of 0.075-0.63 mm; moisture content  $\omega=0.2\%$  ; internal friction angle  $\varphi=36.5^\circ$  ; cohesion  $c=0$  ; external friction angle between retaining wall and sand  $\delta=24.3^\circ$  . In the process of filling sand in the box, the sand is filled in layers with a thickness of 50 cm, the same standard is used for every layered compaction. The test is started after the completion of sand loading and standing for more than 3 hours.

TABLE I  
THE ARRANGEMENTS OF TEST PARAMETERS

Test number	Height of soil (m)	Width of soil (m)	Width to height ratio
1 <sup>#</sup>	0.30	0.12	0.4
2 <sup>#</sup>	0.30	0.15	0.5
3 <sup>#</sup>	0.30	0.18	0.6
4 <sup>#</sup>	0.30	0.21	0.7
5 <sup>#</sup>	0.30	0.24	0.8
6 <sup>#</sup>	0.30	0.30	1.0
7 <sup>#</sup>	0.30	0.36	1.2
8 <sup>#</sup>	0.40	0.16	0.4
9 <sup>#</sup>	0.40	0.20	0.5
10 <sup>#</sup>	0.40	0.24	0.6
11 <sup>#</sup>	0.40	0.28	0.7
12 <sup>#</sup>	0.40	0.32	0.8
13 <sup>#</sup>	0.40	0.40	1.0
14 <sup>#</sup>	0.40	0.48	1.2

This paper mainly analyzes failure characteristics and earth pressure distribution rule of sand in the passive zone against flexible retaining wall with drum deformation. In order to simulate different engineering situations, 14 groups

of soil test are conducted for flexible retaining wall of 300 mm and 400 mm height, in which the width to height ratio is 0.4-1.2. The arrangements of test parameters are shown in Table I.

III. EXPERIMENTAL RESULTS AND ANALYSIS

A. Soil deformation pattern

The sandy soil deformation characteristics under drum deformation pattern was obtained by combined particle image velocimetry technology with GOM Correlate software analysis [19, 20], the displacement of flexible retaining wall with embedded depth of 300 mm and 400 mm is shown in Fig. 5 and Fig. 6, respectively.

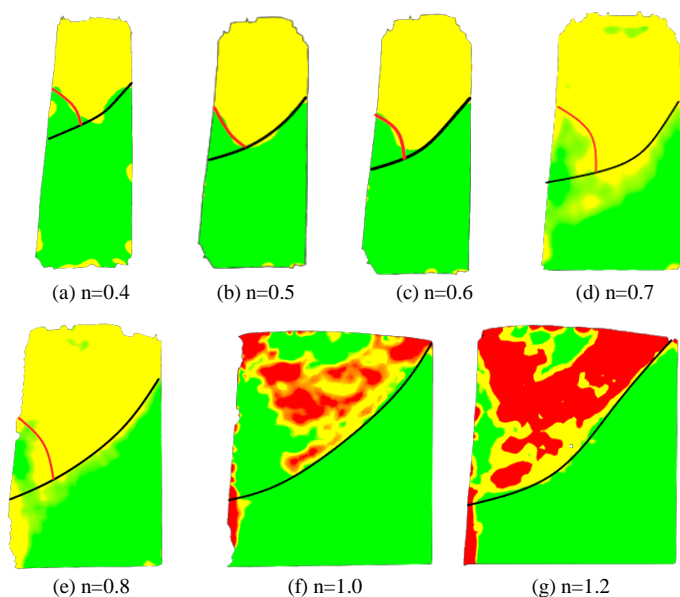


Fig. 5. Displacement of sandy soil under passive limit state for different  $n$  ( $H=300\text{mm}$ )

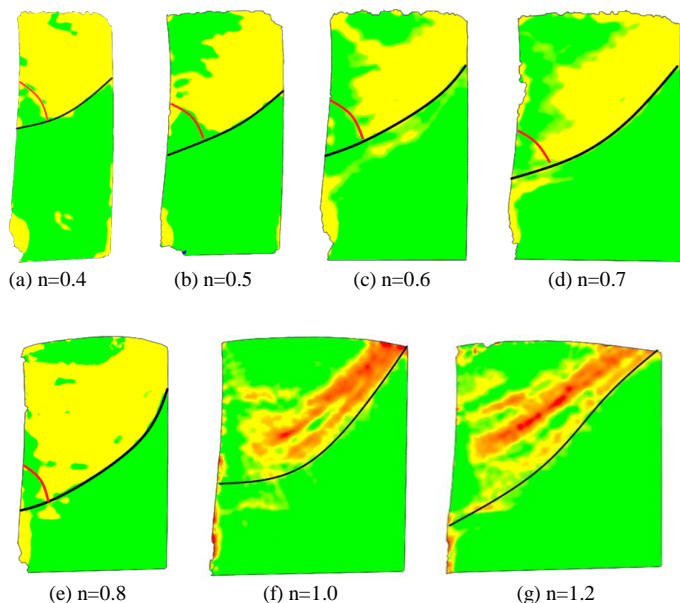


Fig. 6. Displacement of sandy soil under passive limit state for different  $n$  ( $H=400\text{mm}$ )

As shown by the solid black line in Fig. 5 and Fig. 6, the soil sliding fracture surface in the passive zone under the

drum mode is obviously curved, the sliding fracture surface on the side of flexible retaining wall is located in the middle of the soil body; with the increase of width to height ratio, the intersection position of flexible retaining wall and sliding surface gradually moves downward, but it does not develop to the wall heel of flexible retaining wall; On the side of fixed retaining wall, the sliding surface intersects at the middle of fixed retaining wall when the width to height ratio are relatively small, with the increase of width to height ratio, the intersection point of the sliding surface moves gradually upward, when the soil width increases to an infinite continuous state, the sliding fracture surface will slide out at the top of soil mass.

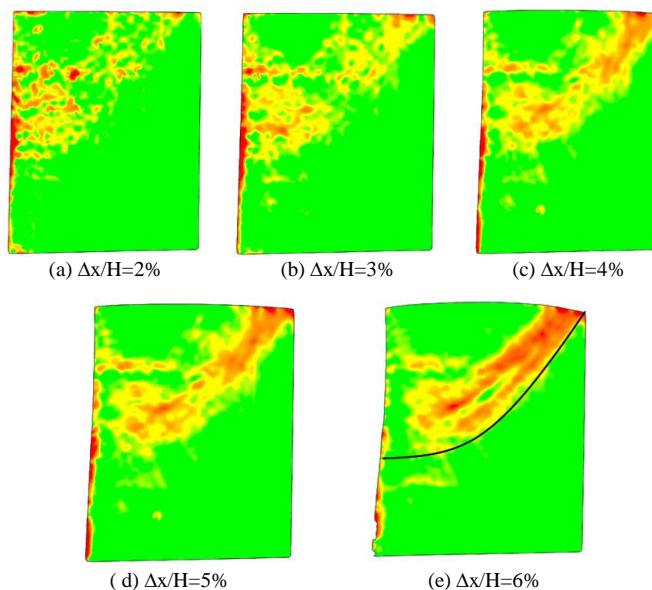


Fig. 7. Displacement fields with sandy soil of different  $\Delta x/H$  for test 13<sup>#</sup>

When sandy soil in the passive zone reaches the ultimate failure state, a continuous slip surface is formed. Fig. 5(f) and Fig. 6(f) indicated the slip crack surface slides out in the top of fixed retaining wall with width to height ratio  $n$  reaches 1.0, therefore, it can be concluded that the critical width to height ratio of finite width to infinite width is  $n = 1.0$  when the passive zone in the vicinity of flexible retaining wall is failure limit state. Fig. 7 shows the displacement development of internal soil mass in the 13<sup>#</sup> test when drum deformation of flexible retaining wall gradually occurs, with the gradual increase of drum deformation displacement, the soil displacement in the passive zone gradually increases accompanied by the top surface of soil mass gradually rises. Finally, a continuous sliding fracture surface is formed in the passive limit state when ratio of maximum horizontal displacement to embedded depth of flexible retaining wall  $\Delta x/H = 6\%$ .

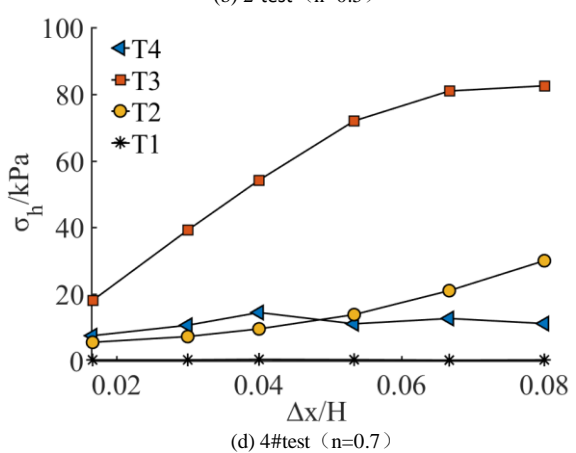
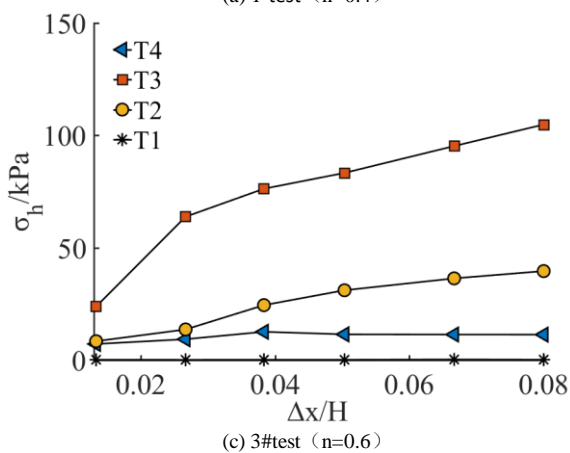
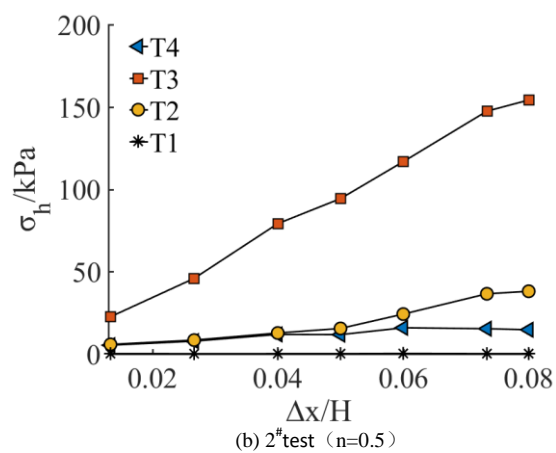
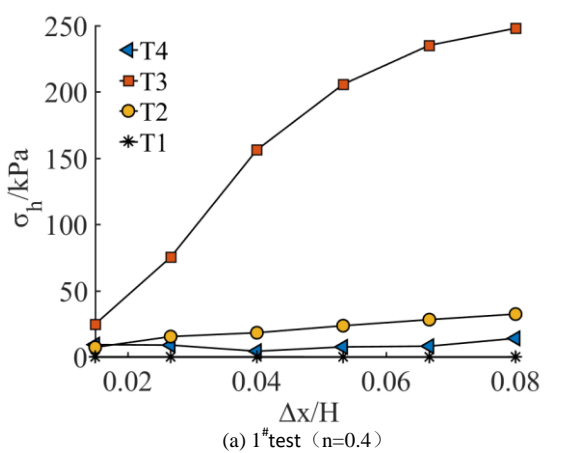
According to the above experimental observation and image analysis, it is considered that sandy soil reaches passive limit state when forming continuous sliding failure surface. For convenience of earth pressure research of flexible retaining wall, the passive earth pressure limit and the maximum horizontal displacement of flexible retaining wall  $\Delta x$  under the passive limit state is measured on the basis

of the standard that forming a continuous sliding failure surface. The maximum horizontal displacement of flexible retaining wall height of 300 mm and 400 mm consistent with passive limit state is 17-22 mm and 21-25 mm, respectively, the ratio of maximum horizontal displacement to embedded depth of flexible retaining wall height of 300 mm and 400 mm consistent with passive limit state is uniformly set to  $\Delta x/H = 7\%$  and  $\Delta x/H = 6\%$ , respectively.

It can also be seen from the displacement deformation diagram that when the load reaches a certain degree, the shear slip surface is formed behind flexible retaining wall; the soil above the sliding surface forms a plastic zone and the soil below the sliding surface is still an elastic zone. The plastic zone has a large displacement and form a large friction resistance at the interface with the flexible retaining wall, at the same time, the soil mass between elastic zone and fixed retaining wall have a certain restriction on the movement of sliding soil mass, forming a vertical soil arch at the bottom of sliding surface [21-22], the part soil of vertical soil arch is wedge-caulking.

*B. Earth pressure on flexible retaining wall*

Fig.8 and Fig.9 show the relationship between horizontal earth pressure  $\sigma_h$  and relative horizontal displacement  $\Delta x/H$  of flexible retaining wall with  $H=300$  mm and  $H=400$  mm, respectively. It can be seen that the distribution and change of earth pressure within the depth range of flexible retaining wall are obviously different; with the increase of horizontal displacement, the earth pressure near the maximum horizontal displacement of flexible retaining wall increases obviously and maintains a large growth trend. As shown in Fig. 8(a), T3 earth pressure gauge is located at the maximum horizontal displacement, the earth pressure increases from 24.76 KPa to 238.39 KPa when the relative horizontal displacement  $\Delta x/H$  vary from 0.015 to 0.7; in addition, the growth trend becomes slow after reaching the limit state. Because the critical width to height ratio of finite width to infinite width is set to  $n = 1.0$ , Fig. 8(f) and Fig. 9(f) is corresponding to the critical state of the transition from finite width to semi-infinite state; It can be seen from the Fig. 8 and Fig. 9 that when the soil transform from critical state to semi-infinite state, the passive earth pressure tends to be stable.



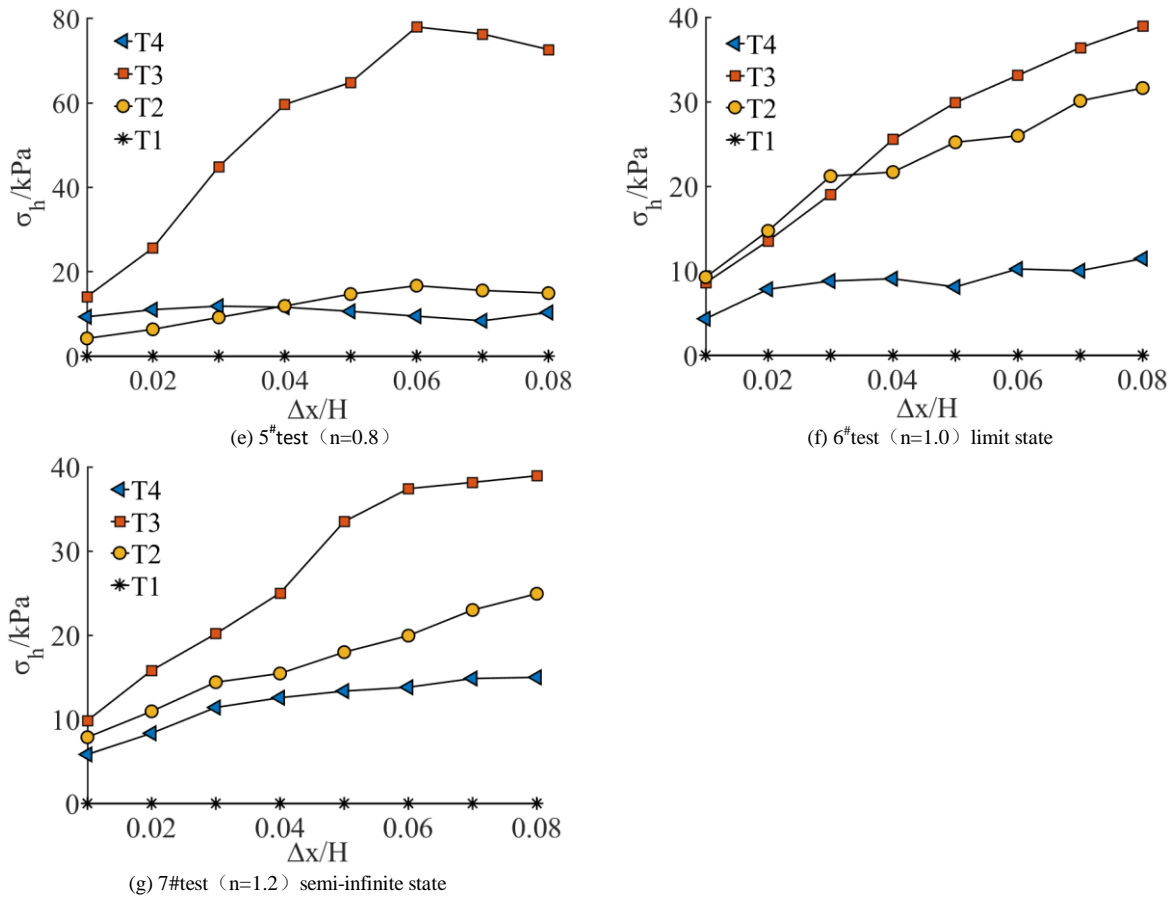
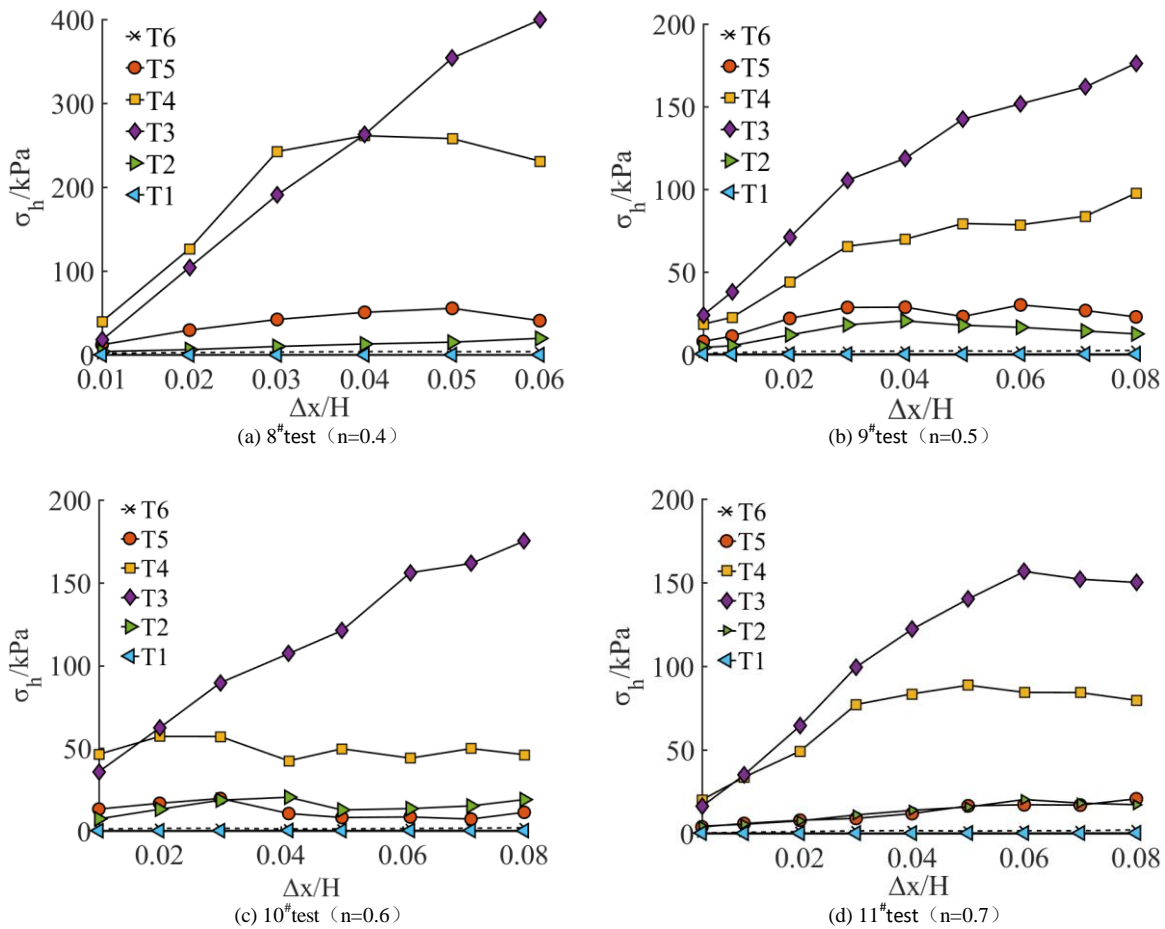


Fig. 8. The curve of lateral earth pressure with the wall movement (H=300mm)



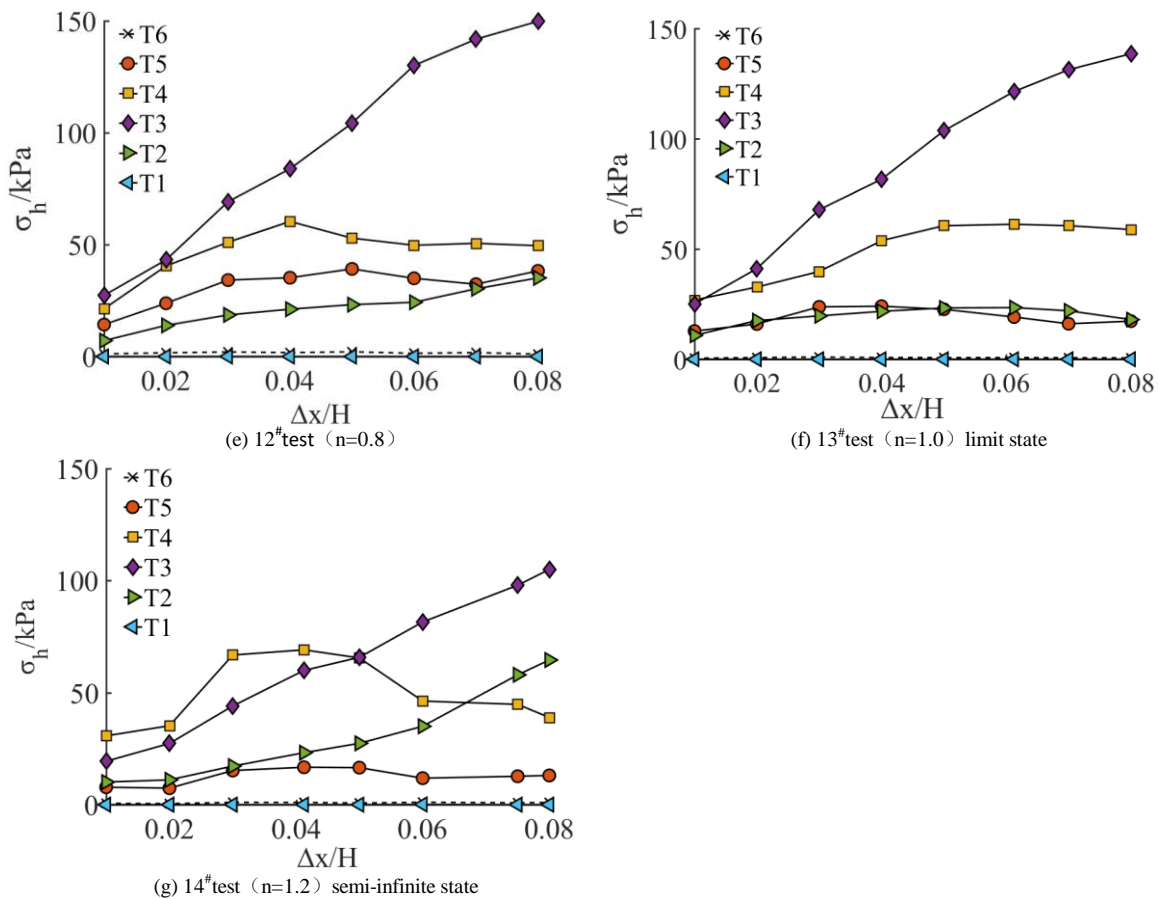
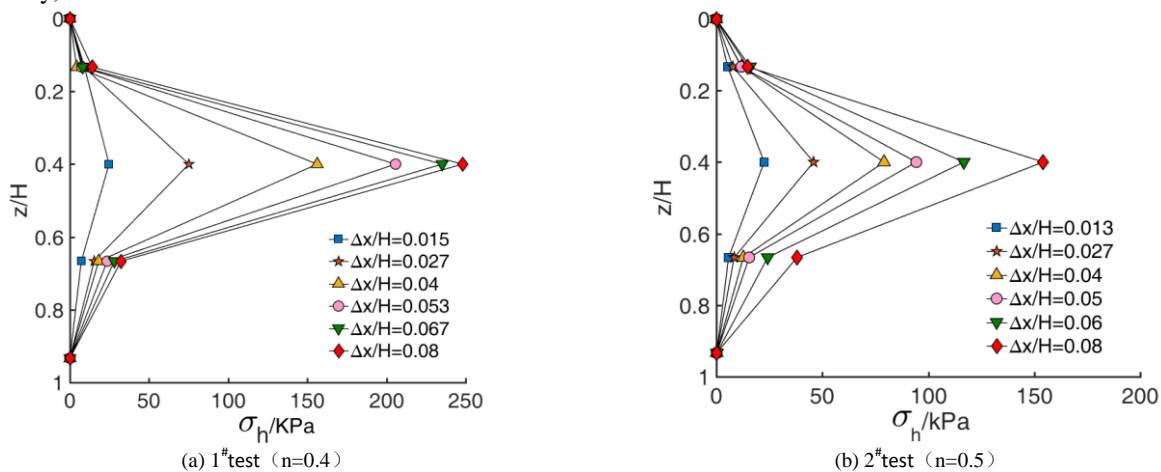


Fig. 9. The curve of lateral earth pressure with the wall movement (H=400mm)

Under different relative displacement  $\Delta x/H$ , the distribution curve of passive earth pressure along relative depth range of the flexible retaining wall for 1<sup>#</sup>-14<sup>#</sup> groups is shown in Fig.10 and Fig.11. When the flexible retaining wall has a drum deformation, the measured passive earth pressure presents a non-linear drum shape distribution. With the increase of depth, the passive earth pressure gradually increases and then decreases rapidly after exceeding the peak value.

In the experiment with same filling soil height, the position of peak passive earth pressure is basically at the same depth. Fig. 10 and Fig. 11 shows that when the height of sand is 300 mm and 400 mm, the position of peak passive earth pressure is mainly located at  $z/H=0.4$  and  $z/H=0.55-0.6$ , respectively; It can be seen that with the increase of

embedded depth of flexible retaining wall, the position of maximum horizontal passive earth pressure moves down under the condition of same width to height ratio; The maximum horizontal displacement of flexible retaining wall is located at the height of 228mm, the position of peak passive earth pressure is slightly lower than the position of maximum horizontal displacement of retaining wall, the main reason is that the uplift of soil beneath the maximum horizontal displacement of flexible retaining wall is restrained and the compaction degree is increased due to the existence of fixed retaining wall, so that the soil strength can be fully exerted.



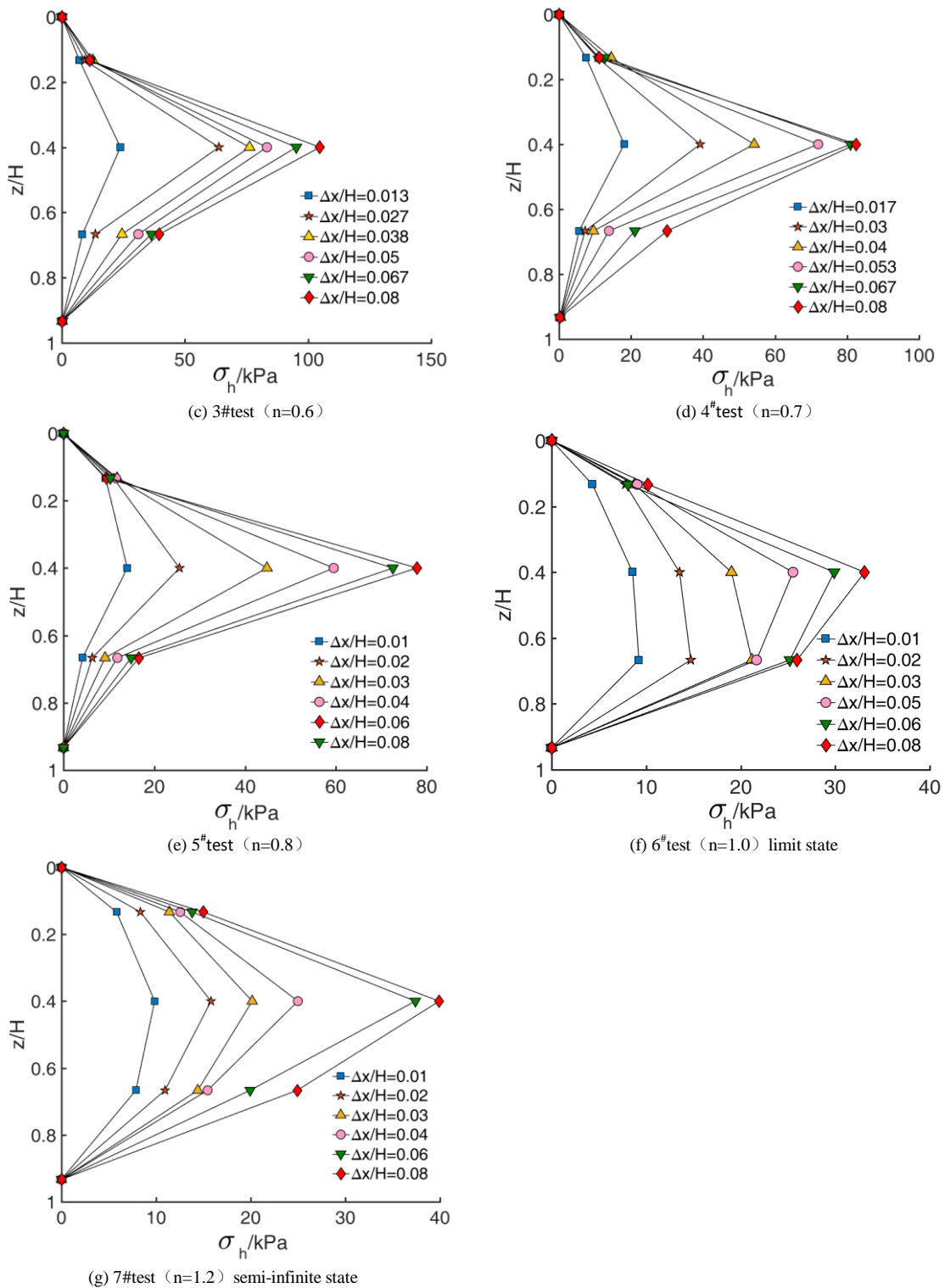
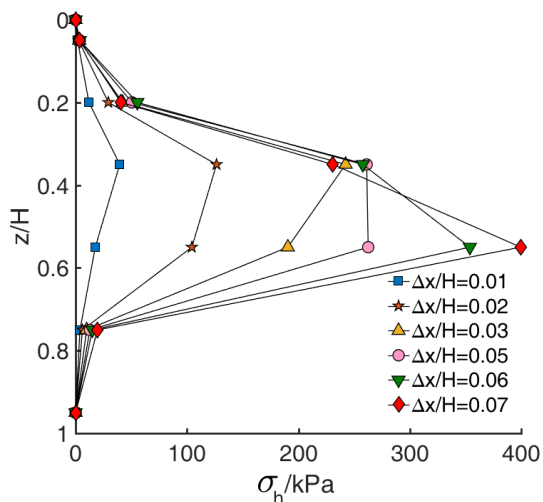
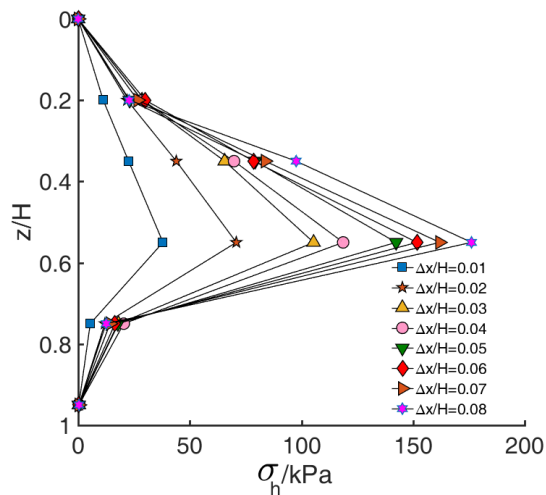


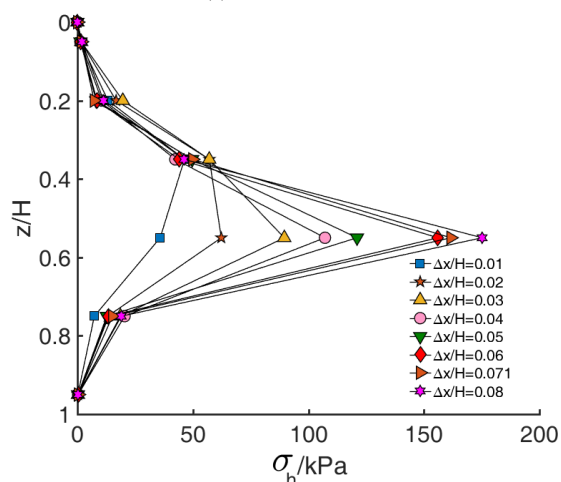
Fig. 10. The curve of lateral earth pressure distribution along relative depth under different displacements (H=300mm)



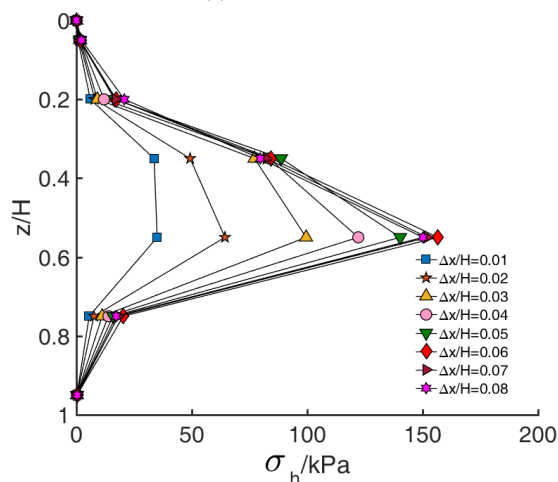
(a) 8<sup>#</sup>test (n=0.4)



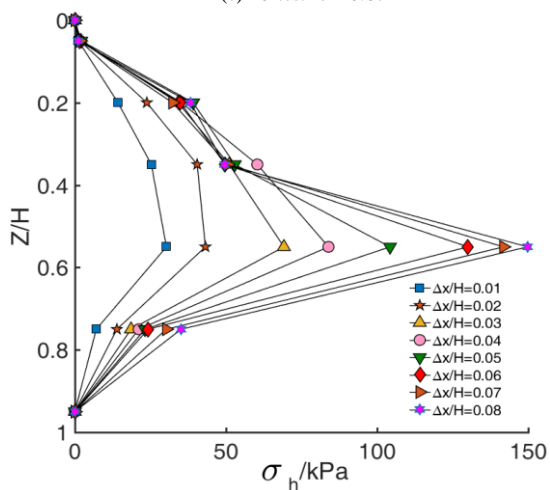
(b) 9<sup>#</sup>test (n=0.5)



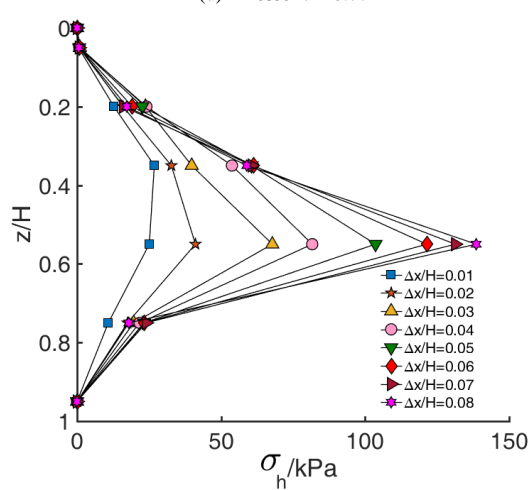
(c) 10<sup>#</sup>test (n=0.6)



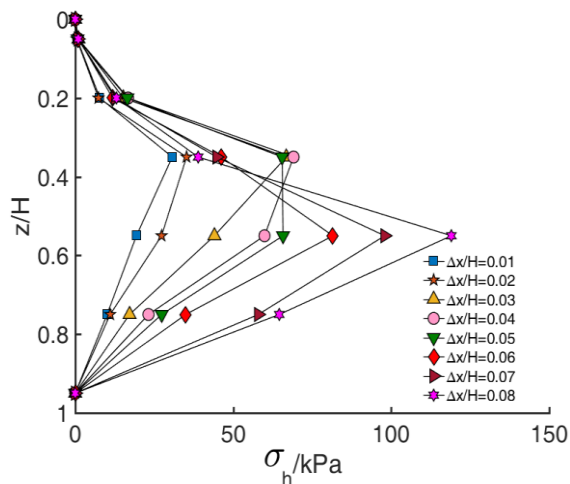
(d) 11<sup>#</sup>test (n=0.7)



(e) 12<sup>#</sup>test (n=0.8)



(f) 13<sup>#</sup>test (n=1.0) limit state



(g) 14<sup>#</sup>test (n=1.2) semi-infinite state

Fig. 11. The curve of lateral earth pressure distribution along relative depth under different displacements (H=400mm)

TABLE II  
PEAK EARTH PRESSURE IN LIMIT STATE  
WITH DIFFERENT EMBEDDING DEPTH (KPa)

Height of filling soil	Width to height ratio n				
	n=0.4	n=0.5	n=0.6	n=0.7	n=0.8
300 mm	238.78	124.43	97.64	80.96	76.22
400 mm	399.49	167.22	156.08	150.66	130.06

Peak earth pressure in limit state with different embedding depth is shown in Table II. If the height of filling soil is 300 mm, the peak value of horizontal earth pressure is 238.78 KPa, 124.43 KPa, 97.64KPa, 80.96KPa and 76.22 KPa when width to height ratio is 0.4, 0.5, 0.6, 0.7 and 0.8; moreover, if the height of filling soil is 400 mm, the peak value of horizontal earth pressure is 399.49 KPa, 167.22 KPa, 156.08KPa, 150.66KPa and 130.06 KPa when width to height ratio is 0.4, 0.5, 0.6, 0.7 and 0.8; therefore, in the limited width range, the measured peak value of horizontal earth pressure increases with the width to height ratio decrease.

Fig. (10) shows that when H=300mm and n=0.4, the peak value of horizontal earth pressure in the limit state is the largest and the measured value is 238.78 KPa, Fig. (11) shows that when H=400mm and n=0.4, the peak value of horizontal earth pressure in the limit state is the largest and the measured pressure is 399.49 KPa; other groups of data showed similar rules, therefore, when width to height ratio remains unchanged, the peak value of passive earth pressure is larger with the greater embedded depth of flexible retaining wall; In the foundation pit, the passive earth pressure is resistant to retaining structure and is beneficial to foundation stability [23-24], therefore, in order to maintain the stability of foundation pit, we should adopt a larger embedded depth in the design of foundation pit.

#### IV. CONCLUSION

By using self-made equipment, the laboratory model tests were carried out to simulate the deformation law of sand and obtain the failure characteristics and passive earth pressure distribution pattern under the drum deformation mode of

flexible retaining wall in long and narrow foundation pit, the main conclusions are drawn as follows:

1) When the passive zone soil behind flexible retaining wall in long and narrow foundation pit reaches the limit state, the sliding fracture presents a continuous and penetrating surface, in which the fracture surface intersects wall body without passing through the heel of flexible retaining wall. With the increase of width to height ratio, the position of sliding surface interface on the side of flexible retaining wall declines and on the side of fixed retaining wall rises.

2) When flexible retaining wall bulges, the distribution of passive earth pressure varies significantly within the depth range, with the increase of horizontal displacement, the earth pressure near the maximum horizontal displacement of flexible retaining wall increases obviously and keeps a large growth rate until reaching the limit state; then, the growth trend slows down after reaching the limit state.

3) When flexible retaining wall has a drum deformation, the measured passive earth pressure presents a non-linear drum shape distribution. Along with the increase of depth, the passive earth pressure gradually increases and then decreases rapidly after exceeding the peak value. with the increase of embedded depth of flexible retaining wall, the position of maximum horizontal passive earth pressure moves down under the condition of same width to height ratio. Besides, because the uplift of soil beneath the maximum horizontal displacement of flexible retaining wall is restrained and the compaction degree is increased due to the existence of fixed retaining wall, the position of the peak passive earth pressure is slightly lower than the position of maximum horizontal displacement of flexible retaining wall.

4) In the limited width range, the measured peak value of horizontal earth pressure increase with the width to height ratio decrease. When the width to height ratio remains unchanged, the peak value of passive earth pressure is larger with the greater embedded depth of flexible retaining wall. In order to maintain the stability of foundation pit, we should adopt a larger embedded depth in the design of foundation pit.

Through the model test on failure characteristics and earth pressure distribution law in the passive zone of flexible support structure, the resultant force and action point of earth pressure in the passive zone can be obtained; the study

provides beneficial reference for the calculation on stability and the embedded depth of support structure.

REFERENCES

[1] K. T. Chau, X. Yang, "Nonlinear interaction of soil-pile in horizontal vibration," *Journal of Engineering Mechanics*, vol. 131, no. 8, pp. 847-858, 2005.

[2] J. He, D.L. Wu, J.S. Ma, H.K. Wang, Y. Li, "Study on the influence law of loading rate on soil pressure bearing characteristics," *Engineering Letters*, vol. 27, no. 4, pp. 724-730, 2019.

[3] V. Greco, "Active thrust on retaining walls of narrow backfill width," *Computers and Geotechnics*, vol. 50, pp. 66-78, 2013.

[4] X.Q. Yu, Z.L. Zhang, W.T. Han, "Experiment measurements of rssi for wireless underground sensor network in soil," *International Journal of Computer Science*, vol. 45, no. 2, pp. 237-245, 2018.

[5] T.S. O'Neal, D.J. Hagerty, "Earth pressures in confined cohesionless backfill against tall rigid walls-a case history," *Canadian Geotechnical Journal*, vol. 48, no. 8, pp. 1188-1197, 2011.

[6] Munadi, I. Solekhuudin, Sumardi, A. Zulijanto, "A numerical study of steady infiltration from a single irrigation channel with an impermeable soil layer," *Engineering Letters*, vol. 28, no. 3, pp. 643-650, 2020.

[7] L.T. Xu, Z.C. Zhang, R.Z. Zhang, J.G. Qian, "Model test on active earth pressure in sand induce by the movement of retaining wall," *Chinese Journal of Underground Space and Engineering*, vol. 13, no.5, pp. 1296-1302, 2017.

[8] Y.Y.Zhou, M.L. Ren, "Experimental research on active earth pressure acting on a rigid wall," *Chinese Journal of Geotechnical Engineering*, vol. 12, no.2, pp. 19-26, 1990.

[9] S.Q.Peng, A.H. Liu, L. Fan, "Active earth pressure for rigid retaining walls with different displacement modes," *Chinese Journal of Geotechnical Engineering*, vol. 31, no. 1, pp. 32-35, 2009.

[10] W.Timpitak, N. Pochai, "Numerical simulations to a one-dimensional groundwater pollution measurement model through heterogeneous soil," *International Journal of Applied Mathematics*, vol. 50, no. 3, pp. 558-565, 2020.

[11] H.W. Ying, W.Zhu, B.B. Zheng, "Calculation and distribution of active earth pressure against flexible retaining walls," *Chinese Journal of Geotechnical Engineering*, vol. 36, no. supp2, pp. 1-6, 2014.

[12] H.W. Ying, Q.P. Cai, "Distribution of active earth pressure against flexible retaining walls with drum deformation," *Chinese Journal of Geotechnical Engineering*, vol. 30, no. 12, pp. 1805-1810, 2008.

[13] R.M. Peng, Q.L. Ji, "Dynamic passive earth pressure on retaining wall under various modes of movement," *Rock and Soil Mechanics*, vol. 30, no. supp2, pp. 34-38, 2009.

[14] W.A. Take, A.J. Valsangkar, "Earth pressures on unyielding retaining walls of narrow backfill width," *Canadian Geotechnical Journal*, vol. 38, no. 6, pp. 1220-1230, 2001.

[15] M.H. Khosravi, T. Pipatpongsa, J. Takemura, "Experimental analysis of earth pressure against rigid retaining walls under translation mode," *Geotechnique*, vol. 63, no. 12, pp. 1020-1028, 2013.

[16] R.Q. Xu, Y.K. Cheng, Z.X. Yang, "Experimental research on the passive earth pressure acting on a rigid wall," *Chinese Journal of Geotechnical Engineering*, vol. 24, no. 5, pp. 570-575, 2002.

[17] H.W. Ying, J.H. Zhang, X.G. Wang, "Experimental analysis of passive earth pressure against rigid retaining wall under translation mode for finite soils," *Chinese Journal of Geotechnical Engineering*, vol. 38, no. 6, pp. 978-986, 2016.

[18] W. Zhu, "Experimental and theoretical study on earth pressures considering limited soil sand retaining wall deformation," Hangzhou: Zhejiang University, 2014.

[19] M. Niedostatkiewicz, D. Lesniewska, J. Tejchman, "Experimental analysis of shear zone patterns in cohesionless for earth pressure problems using particle image velocimetry," *Strain*, vol. 47, no. supp2, pp. 218-231, 2011.

[20] M.H. Khosravi, T. Pipatpongsa, J. Takemura, "Experimental analysis of earth pressure against rigid retaining walls under translation mode," *Géotechnique*, vol. 63, no. 12, pp. 1020-1028, 2013.

[21] W.D. Hu, L.X. Zeng, X.H. Liu., "Active earth pressures against rigid retaining walls for finite soil in grading condition," *Hydrogeology & Engineering Geology*, vol. 45, no. 6, pp. 63-70, 2018.

[22] M.H. Yang, L.C. Wang, M.H. Zhao, "Calculation of active earth pressure for finite soils based on the soil arching theory," *Building Structure*, vol. 43, no. 2, pp. 71-75, 2013.

[23] T.C Han, L.X. Xie, Z. Liu, "Calculation of passive earth pressure for finite soil in foundation pit under pit-in-pit condition," *Rock and Soil Mechanics*, vol. 39, no. 12, pp. 4404-4412, 2018.

[24] G. Wei, J.T. Zheng, "Calculated method of passive earth pressure in deep pit engineering considering excavation effect," *Chinese Journal of Geotechnical Engineering*, vol. 28, no. sup 1, pp. 1493-1496, 2006.



**Mr. Xinnian Zhu** was born in November 1975 and received his B.E.degree and M.S.Degree from Hunan University, Changsha, China, in 1999 and 2010, respectively. His research interests are mainly on slope support and earth pressure test for foundation pit engineering. Xinnian Zhu has worked as a lecturer in Hunan Institute of Science and Technology. He has authored or co-authored 5 journal papers and 2 international conference papers to date.



**Dr. Yongqing Zeng** was born in February 1991 and received his M.S.Degree from Anhui University of Science and Technology, Huainan, China, in 2016, and received the Ph.D. degree from Institute of Rock and Soil Mechanics, Chinese Academy of Sciences, Wuhan, China, in 2019. Yongqing Zeng has worked as a lecturer in Hunan Institute of Science and Technology. He authored or co-authored 15 journal papers and 4 international conference papers to date.



**Dr. Weidong Hu** received the Ph.D. degree from Hunan University, Changsha, China, in 2016. Hu is the professor of College of Civil Engineering and Architecture, Hunan Institute of Science and Technology, Yueyang, China. His research interests cover excavation engineering and earth pressure. He has published more than 40 technical papers.



**Dr. Xiaohong Liu** received the Ph.D. degree from Central South University, Changsha, China, in 2011. She is the professor of College of Civil Engineering and Architecture, Hunan Institute of Science and Technology, Yueyang, China. Her research interests cover excavation engineering and earth pressure and non-contact testing of foundation deformation. She has published more than 30 technical papers.



**Xiyu Zhou** was born in August 1998 and received his B.E.degree from Hunan Institute of Science and Technology, Yueyang, China, in 2019. His research interests are mainly on slope support and earth pressure test for foundation pit engineering. Xiyu Zhou has worked as an assistant engineer in China Railway Major Bridge Engineering Group Limited Company. He has authored or co-authored 2 journal papers.